Received: 10 September 2019 | Revised: 11 February 2020 | Accepted: 16 February 2020

DOI: 10.1002/app.49166

ARTICLE

Applied Polymer SCIENCE WILEY

Influence of monomeric concentration on mechanical and electrical properties of poly(styrene-*co*-acrylonitrile) and poly(styrene-*co*-acrylonitrile/acrylic acid) yarns electrospun

Rubén Caro-Briones[1] | **Blanca Estela García-Pérez**[2] | **Héctor Báez-Medina**[3] | **Eduardo San Martín-Martínez**[4] | **Gabriela Martínez-Mejía**[2] | **Rogelio Jiménez-Juárez**[2] | **Hugo Martínez-Gutiérrez**[5] | **Mónica Corea**[1]

[1]Escuela Superior de Ingeniería Química e Industrias Extractivas, Instituto Politécnico Nacional, Av. Luis Enrique Erro S/N, Unidad Profesional Adolfo López Mateos, Zacatenco, Ciudad de México, México

[2]Escuela Nacional de Ciencias Biológicas, Instituto Politécnico Nacional, Unidad Profesional Lázaro Cárdenas Prolongación de Carpio y Plan de Ayala S/N Col. Santo Tomas, Ciudad de México, México

[3]Centro de Investigación en Computación, Instituto Politécnico Nacional, Av. Juan de Dios Bátiz, Esq. Miguel Othón de Mendizábal, Col. Nueva Industrial Vallejo, Ciudad de México, México

[4]Centro de Investigación en Ciencia Aplicada y Tecnología Avanzada, Instituto Politécnico Nacional, Ciudad de México, México

[5]Centro de Nanociencias y Micro-Nanotecnologías, Instituto Politécnico Nacional, Av. Luis Enrique Erro S/N, Unidad Profesional Adolfo López Mateos, Zacatenco, Ciudad de México, México

Correspondence
Mónica Corea, Escuela Superior de Ingeniería Química e Industrias Extractivas, Instituto Politécnico Nacional, Av. Luis Enrique Erro S/N, Unidad Profesional Adolfo López Mateos, Zacatenco, Alcaldía Gustavo A. Madero, C.P. 07738, Ciudad de México, México.
Email: mcoreat@yahoo.com.mx, mcorea@ipn.mx

Hugo Martínez-Gutiérrez, Centro de Nanociencias y Micro-Nanotecnologías, Instituto Politécnico Nacional, Av. Luis Enrique Erro S/N, Unidad Profesional Adolfo López Mateos, Zacatenco, Alcaldía Gustavo A. Madero, C.P. 07738, Ciudad de México, México.
Email: humartinez@ipn.mx

Funding information
Consejo Nacional de Ciencia y Tecnología (CONACYT), Grant/Award Number: 596936; Secretaria de Investigación y Posgrado, Instituto Politécnico Nacional, Grant/Award Numbers: 20196644, 20195353

Abstract

Two series of copolymers were synthesized by emulsion polymerization: poly(styrene-*co*-acrylonitrile) P(S:AN) and P(S:AN-acrylic acid) P(S:AN-AA). The monomeric concentrations in both series were: 0:100, 20:80, 40:60, 50:50 (wt%:wt%), and 1 wt% of AA. The copolymers were dissolved in *N*,*N*-dimethylformamide (4–10 wt%) and were electrospun. Polymeric yarns were collected using a blade collector. The synthesized and fabricated materials were characterized by known techniques. Mechanical and electrical properties of polymeric yarns indicated a dependence of monomeric concentration. Elastic modulus increases as acrylonitrile concentration increases (up to 30 MPa). Yarns were submitted to degradation process into saline solution, where the acrylic acid content kept a constant elastic modulus at long times. The electrical current into yarns was higher when the concentration is 50:50 wt%:wt% (1.2 mA). The cytotoxicity results showed a cell viability close to 100% for yarns without AA.

KEYWORDS
conducting polymers, electrospinning, sensors and actuators

1 | INTRODUCTION

In recent years, the biomimetic actuators development has increased attention, in particular for artificial muscles. They can be made from polymers, metallic and composite materials.[1–4] Research and development of diverse materials for design of artificial muscles have been reported moreover, these materials present mechanical limitations, for example low elastic modulus.[5] For this reason, further investigations are necessary to develop new materials with useful electrical and mechanical properties.

An artificial muscle is defined as a class of material or device that can reversibly contract, expand, rotate, or combine motions, within one component. This movement as consequence of an external stimulus such as voltage, current, pressure, temperature, light, and so forth.[6,7]

The polymers are considered as a promising material to obtain versatile mechanical and electrical properties. The mechanical properties are brought about by chemical and physical tailor-made structure, meanwhile the electrical are obtained from the chemical arrangement into polymer chain. A chemical arrangement can be achieved as result of copolymers synthesis design where, specific functional groups react with the polymer backbone.[8,9] For example, polyaniline (PANi) presents a semiconductor behavior due to internal redox process. That means, the free electrons dislocation along the polymer chain produces an electrical current.[10,11] For this reason, polymeric yarns structure is shown as a good candidate to develop artificial muscles, because of the hierarchically complex interior architectures can result in superior mechanical, chemical, or anisotropic properties.[12–14]

Some works have reported artificial muscle made from synthetic polymers. For example, Fujisue et al. developed a soft actuator mimicking natural muscles using flexible conducting polypyrrole (PPy) films moved by electrical stimulus applied.[1] Other research was done by Bassil et al. who fabricated artificial muscles from polyacrylamide gel fibers. The materials were cylindrical gel with 16.5 mm of length. The samples were immersed in NaCl 9% solution and a voltage of 5 V applied, then the gel shrinks by releasing swelling agent (H_2O), contracting almost 37% of its initial value.[2] Choe et al. researched the volume deformation of commercial PAN fibers at different pHs. A polyacrylonitrile (PAN) yarn fiber gel with initial diameter of 30 μm was fabricated and submerged in a 1 M hydrochloric acid solution and a current of 80 μA was applied. The results showed diameter decreased up to 14 μm; meanwhile, when the materials were submerged in a 1 M lithium hydroxide solution, diameter increased to 40 μm.[3] An artificial muscle from cross-linked poly(ethylene-*co*-vinyl acetate) fibers was fabricated by Fan et al. These fibers exhibited a maximum actuation strain of 68%, when a heating was applied (up to 67°C). The performance muscle is tunable at $20 < T/°C < 70$.[4]

Electrospinning is a versatile, low-cost, and practical technique for fabricating microscale and nanoscale fibers. The process uses a polymeric solution or polymeric melt into a glass syringe and a syringe pump displaces it, until obtain a polymeric solution drop at needle tip.[15] A high voltage is applied between the needle tip and collector. Due to strength of electric field, surface tension of polymeric solution decreases and results in a cone shape (Taylor's cone), which ejects a charged polymer jet. The electrical forces, elongate the jet and reduce the fiber diameter, the material is deposited on the grounded collector.[15–17]

The fibers morphology is influenced by different parameters as: (a) polymeric solution (concentration, molecular weight, viscosity, surface tension, electrical constant, and conductivity); (b) process settings (voltage applied, work distance, feed rate, and collector type); and (c) ambient conditions (temperature and relative humidity).[18] Configuration parameters allow to control the structure and therefore fabricate tailor-made fibers.[18–20]

There is a wide range of synthetic polymers used in electrospinning technique as: poly(vinyl alcohol), PANi, poly(lactide-*co*-glycolide), poly(ethylene glycol), polystyrene (PS), polyacrylonitrile (PAN), among others, and natural polymer such as chitosan, alginate, cellulose, or collagen are also used. They have been reported with a great potential and useful for several applications such as antibacterial, photocatalyst, sensing, electronic devices, energy store, filtration, and biomedical applications (tissue engineering scaffolds, drug delivery, grafts, and artificial muscles).[4,20–38]

Several works have reported the use of commercial polymers and preparation of polymeric solutions by mechanical methods for yarns fabrication. However, the chemical design for polymer tailor-made allows enhancing mechanical and electrical properties. For that emulsion, polymerization techniques can be used to modify the morphology particle, polymer phases, location of functional groups into polymeric backbone and the composition of monomers into the copolymer chain.[39,40]

In this work, two series of copolymers tailor-made of P(S:AN) and P(S:AN-AA) at several compositions were synthesized by emulsion polymerization techniques. The obtained materials were characterized by dynamic light scattering (DLS) and scanning electron microscope

(SEM). Polymeric solutions were prepared with *N*,*N*-dimethylformamide (DMF) and their rheological properties measured. The materials were electrospun to produce fibers and yarns. The mechanical (elastic modulus) and electrical properties of yarns were measured. The yarns were submitted to a degradation process during 1 month in saline solution, taking samples at several times to evaluate again their mechanical properties. Cytotoxicity analysis of yarns on macrophage cells was also investigated.

2 | EXPERIMENTAL

2.1 | Materials

Styrene (Mw~104.15 g/mol), acrylonitrile (Mw~53.06 g/mol), DMF (Mw~73.09 g/mol), acrylic acid (Mw~72.06 g/mol), and sodium persulfate (Mw~238.10 g/mol) were purchased from Sigma-Aldrich, St. Louis, MO. Surfactant IGEPAL CA-630 from SOLVAY. Deionized water from Meyer, Mexico. Buffer solution (biphthalate), pH 4, buffer solution (phosphate), pH 7 and buffer solution (borate), pH 10 from J. T. Baker, Mexico. Deuterated dimethyl sulfoxide (DMSO-d_6) from Cambridge Isotope Laboratories, Inc. 3-(4,5-Dimethylthiazol-2-yl)-2,5-diphenyltetrazolium bromide (MTT) from Sigma Chemical, MA. Murine macrophage cell line J774A.1 from American Type Culture Collection (ATCC TIB-67). Dulbecco Modified Eagle Medium (DMEM/F12), gentamycin and penicillin from Sigma-Aldrich. Fetal bovine serum (FBS) and Hyclone Laboratories Inc. Logan, UT. All materials were used without further purification.

2.2 | P(S:AN) concentration gradient nanoparticles synthesis

Two series of copolymer with different ratio concentrations were synthesized. The first one was P(S:AN) 0:100, 20:80, 40:60, and 50:50 (wt%:wt%), while the second one was P(S:AN-AA) 0:100–1, 20:80–1, 40:60–1, and 50:50–1 (wt%:wt%-wt%). The reaction was carried out by emulsion polymerization technique in a semi-continuous process at power feed conditions.[41] In this way, a gradient of concentration inside the particles was generated. The formulation used to prepare 100 g of latex with a solid content of 40 wt% is shown in Table 1.

The synthesis system consisted in two addition tanks connected in series to 1 L stirred glass reactor with a condenser under a dynamic flow of nitrogen. The temperature was maintained at 75°C controlled by a thermal bath and stirring rate was fixed at 300 rpm. A scheme of polymerization process is shown in Figure 1.

TABLE 1 Formulation 100 g of latex, ratio concentration 50:50–1% wt%:wt%-wt%

Component	Main reactor (g)	Addition Tank 1 (g)	Addition Tank 2 (g)
Solution surfactant 0.5 wt%	0.60		
Solution surfactant 3.73 wt%		13.00	7.00
Styrene (S)		20.00	
Acrylonitrile (AN)			19.60
Acrylic Acid (AA)			0.40
Solution initiator 2.0 wt%	1.20	4.20	2.00
Deionized water	32.00		

2.3 | Latex characterization

2.3.1 | Dynamic light scattering

The distribution particle diameter of polymeric particles was measured using a Zetasizer Nano ZSP (Malvern Instruments, UK). The samples were diluted at 10 ppm with deionized water. The measurements were made by quadruplicate at 25°C.

The average particle diameters were calculated using Equation (1).

$$\bar{D}_Z = \frac{\sum n_i D_i^5}{\sum n_i D_i^4} \tag{1}$$

The polydispersity index (PDI) was calculated using Equations (2)–(4).

$$\bar{D}_n = \frac{\sum n_i D_i}{\sum n_i} \tag{2}$$

$$\bar{D}_w = \frac{\sum n_i D_i^4}{\sum n_i D_i^3} \tag{3}$$

$$\mathrm{PDI} = \frac{D_w}{D_n} \tag{4}$$

where n_i is the number of particles with diameter D_i, as function of size (Z), number (n), and weight (w).

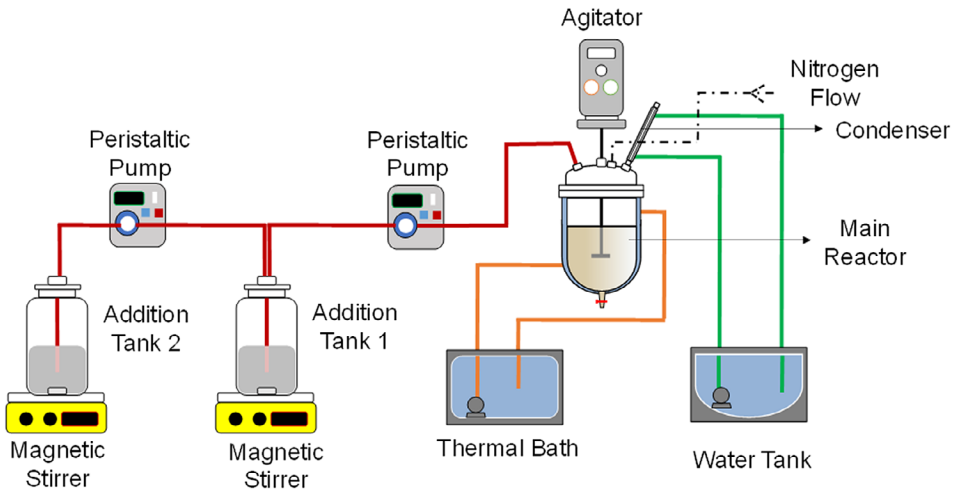

FIGURE 1 Synthesis semicontinuous system [Color figure can be viewed at wileyonlinelibrary.com]

2.3.2 | Scanning electron microscopy

The morphology and diameter of polymeric particles were observed with an SEM (JEOL JSM - 7800F, Tokyo, Japan) at 5 kV and work distance of 3.0 mm. The latex samples were diluted at 10 ppm with deionized water. Deposited on aluminum foil and dried at room temperature.

2.4 | Electrospinning process

2.4.1 | Preparation of polymer solutions

A sample of 1 g of polymer was weighted and dissolved in 10 g of DMF (dielectric constant of $\varepsilon = 37.66$) by mechanical stirring for 12 hr at room temperature.[42] Four concentrations of polymeric solutions were prepared: 4, 6, 8, and 10 wt%.

2.4.2 | Rheological properties

The rheological properties of polymeric solutions were measured using a Modular Compact Rheometer MCR 502 (Anton Paar, Graz, Austria) on rotation mode. A 1.5 ml sample of spinning solution was deposited onto rheometer base and the plane plate geometry (25 mm diameter, 0°) was collocated at 1 mm above the base. Measurements of viscosity were made from 30 to 120°C at a scanning rate 2°C/min.

2.4.3 | Fiber fabrication

The spinning solutions were placed into a 5 ml glass syringe connected to a metallic 21 G needle through PTFE tubing. The needle and the collector were connected to high voltage power supply. The applied voltage was set at 18 kV. The solutions were fed at 2.5 ml/hr by syringe pump. The electrospun fibers or yarns were collected for 10 min on a blade collector, which was placed 5 cm from the needle tip. The obtained fibers were dried by 1 hr at 60°C. All solutions were electrospun under same conditions.

2.5 | Fiber characterization

2.5.1 | Scanning electron microscopy

The morphology and diameter of fibers and yarns were observed in an SEM (JEOL JSM - 7800F) at 2 kV and work distance of 9.5 mm. The samples were dried at 60°C and coated with gold by sputtering.

2.5.2 | Mechanical properties

A texture analyzer (TA.X2i, UK) was used to test the elasticity modulus of polymeric yarns. Samples of 6 cm length were analyzed by quadruplicate at test speed of 1 mm/s, using a 25 kg load cell and a sensitivity at 0.10 N.

2.5.3 | Electrical properties

A DC Probe Station MST 5500 (MSTECH, Korea) was used to analyze the current–voltage relation in polymeric yarns. The yarns tips were covered with gold by sputtering to be used as contacts. Yarns of 4 cm length were moistened into 10 ml saline solution and evaluated at different pHs (4, 7, 10) using buffer solutions. The

yarns were tested from 0 to 10 V and the experiments were made by triplicate at room temperature.

2.5.4 | ^{1}H NMR and ^{13}C NMR

One-dimensional ^{1}H-NMR and ^{13}C-NMR spectra were recorded at 600 MHz on a Bruker AVANCE III (Bruker BioSpin, DE). The submerged samples of PAN yarns into saline solution at different periods of time (0, 1, 5, 10, and 15 days) were washed with deionized water and dried at 40°C during 2 hr. The polymers were dissolved in DMSO-d_6. As a reference for the ^{1}H NMR chemical shifts, the signals of nondeuterated solvent residues were set at $\delta = 2.5$ and 3.33 ppm for DMSO and water, respectively. For ^{13}C NMR, the signal was set at $\delta = 39.52$ ppm for DMSO.

2.5.5 | Cytotoxicity test

The cytotoxicity of copolymer yarns was tested using MTT and SpectraMax M3 Microplate reader (Molecular Devices, CA). Yarn samples of 1 cm length were placed in a 24-well plate, which was sterilized with 100 µl of ethanol during 2 hr and ultraviolet light for 30 min. The procedure was repeating twice.

The assay was performed with murine macrophage cell line J774A.1 and maintained with DMEM/F12, supplemented with 10% FBS, gentamycin (25 mg/ml), and penicillin (50,000 U/ml) at 37°C in an atmosphere of 5 vol% CO_2.

Macrophage cells (200,000/1 ml) were added to each 24-well plate containing the P(S:AN) and P(S:AN-AA) yarns. As a control, cells without copolymers yarns were also evaluated. The samples were incubated at 37°C with 5 vol% CO_2 atmosphere. Once the incubation time was over ($t = 24$ hr), 100 µl of 1 mg/ml MTT solution was added to each microwell and incubated for 3 hr. Subsequently, the MTT solution was removed and 200 µl of DMSO was added to solubilize the formazan precipitates. Finally, the absorbance was quantified at a wavelength of 570 nm in a SpectraMax M3 Microplate reader. In order to calculate the cell viability percentage, the corresponding absorbance to cells without the copolymers was taken as 100% of cell viability.

3 | RESULTS AND DISCUSSION

Two series of latex with different proportions of monomers were obtained by means of emulsion polymerization techniques in a power feed semicontinuous process. The monomers ratio composition were (S:AN): 0:100, 20:80, 40:60, and 50:50 wt%:wt%. The first one (Series *A*) contained styrene and acrylonitrile, while the second one (Series *B*) 1 wt% of acrylic acid was also added.

The synthesized materials were characterized by DLS except to the polymer with 100% AN, which was measured with a Vernier instrument (Mitutoyo, model 505, Japan). The average particle size ($\bar{D}_Z$) was calculated from distribution particle size data and using Equation (1). The results of average particle diameter and PDI are shown in Table 2 for both series (see Supporting Information, Figures S1 and S2).

Representative SEM micrographs for Series *A* and *B* particles with different monomer ratio concentrations are shown in Figure 2. Figure 2a,c,e corresponds to P(S:AN) 20:80, 40:60, and 50:50 wt%:wt%; meanwhile, Figure 2b,d,f corresponds to P(S:AN-AA) 20:80–1, 40:60–1, and 50:50–1 wt%:wt%-wt%, respectively.

The SEM micrographs reveal a smooth surface, homogeneous and spherical shape of the particles with just styrene and acrylonitrile, while the particles with extra 1 wt% of acrylic acid show a roughness and spherical structure similar to raspberry. Phases contrast is observed between styrene center (darker) and acrylonitrile/acrylic acid lumps all around it (brighter). Raspberry morphology particles show a core particle and small particles anchored into it, attributed to interactions acid–base, hydrogen bonding, covalent bonding, or electrostatic interactions.[43–45]

It has reported that AA is associated with lumps on the surface of polymeric particles, because hydrophilic molecules are usually located on the surface and they can improve the monodispersity and stability of growing particle.[46,47]

The measured diameters from SEM show the same tendency than those measured by DLS technique, a particle diameter increment as AN content increase; however, the obtained diameters by SEM resulted to be smaller than DLS. This is because SEM measurements should be sensitive only to the polymer particles. DLS measurements are sensitive to the hydrated layer on the surface of the nanoparticles in aqueous medium.[46] Micrographs also present two particle sizes to Series *A*; one of them at values close to 500 nm, which means a bimodal population that corresponds to results calculated for PDI (see Table 2).

On the other hand, the raspberry morphology is resulted of reactivity ratio polymer–polymer in the chemical arrangement, which plays a role structuring a continuous polymeric phase. This mean, improve the miscibility of components (PAN, PS, and AA) in the polymeric solution. This has as consequence notorious changes in mechanical behavior of electrospun fibers,

TABLE 2 Average diameter and PDI for P(S:AN) and P(S:AN-AA) nanoparticles

P(S:AN) (wt%:wt%)	$\bar{D}_Z$ (nm)	Polydispersity index	P(S:AN-AA) (wt%:wt%-wt%)	$\bar{D}_Z$ (nm)	Polydispersity index
0:100	3.1×10^6	—	0:100–1	2.86×10^6	—
20:80	967	1.63	20:80–1	855	1.20
40:60	485	2.35	40:60–1	455	1.11
50:50	225	2.21	50:50–1	568	1.03

Abbreviations: PDI, polydispersity index; P(S:AN), poly(styrene-*co*-acrylonitrile); P(S:AN-AA), P(S:AN-acrylic acid).

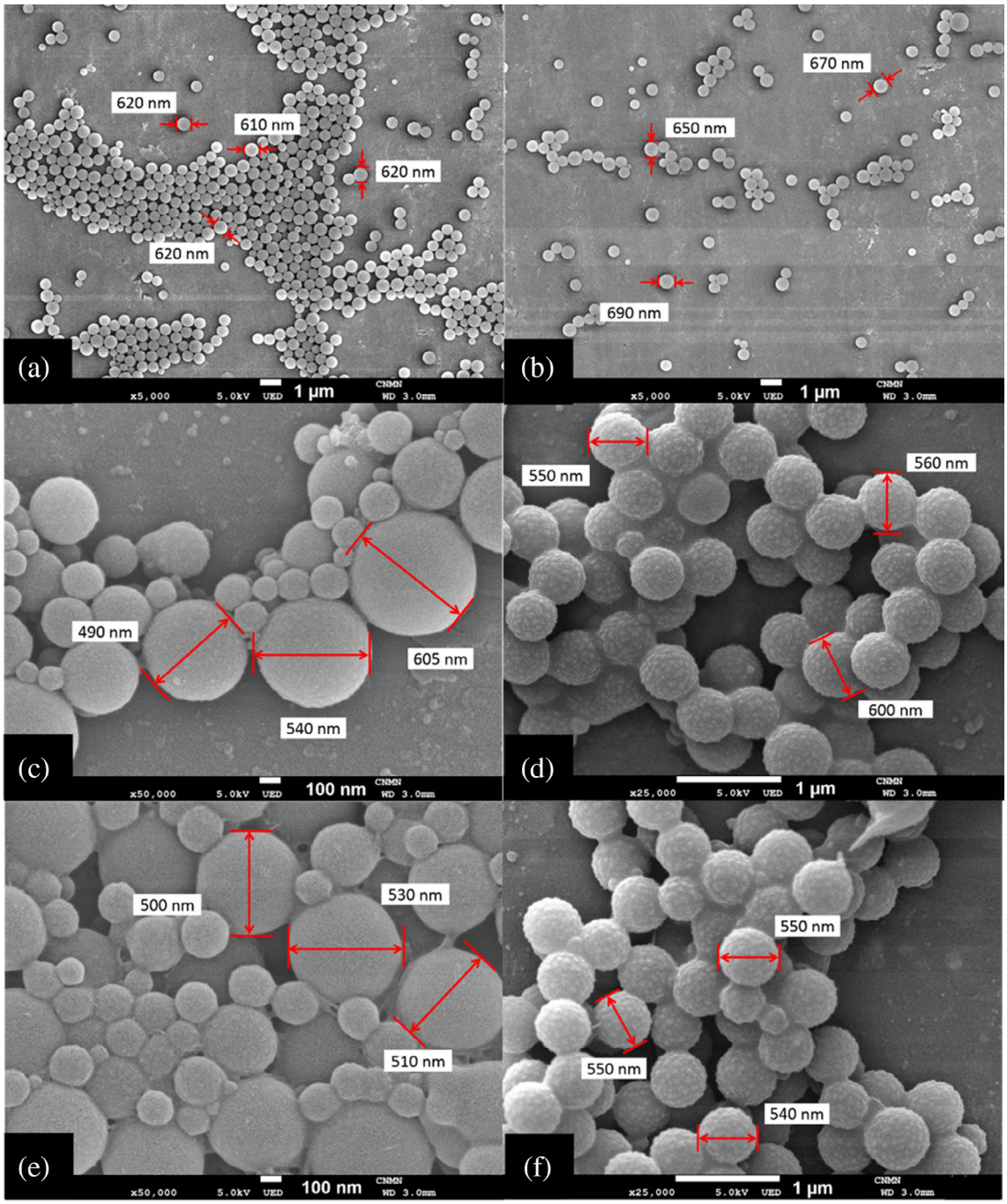

FIGURE 2 Scanning electron microscope (SEM) micrographs of poly(styrene-*co*-acrylonitrile) P(S:AN) wt%:wt% and P(S:AN-acrylic acid) P(S:AN-AA) wt%:wt%-wt% particles with different concentrations: (a) 20:80, (b) 20:80–1, (c) 40:60, (d) 40:60–1, (e) 50:50, and (f) 50:50–1 [Color figure can be viewed at wileyonlinelibrary.com]

where properties as flexibility and elasticity are obtained.[48,49]

In order to prepare the yarns, four polymeric solutions of each material were prepared with DMF at different contents of polymer (4, 6, 8, and 10 wt%). The viscosity (η) of polymeric solutions was measured in a MCR 502 rheometer from 30 to 120°C with a scanning rate of 1°C/min. The measurements were made by triplicate. Figure 3 shows the viscosity as a function of temperature of four polymeric solutions of P(S:AN) with 0:100 and 20:80 wt%:wt% as example, because all materials presented the same behavior.

It is observed that highest viscosity corresponds to the polymeric solution with highest solids content (10 wt%). In addition, η for the P(S:AN) with a composition 0:100 wt%:wt% is kept constant at 10.5 Pa·s (±2 Pa·s) until 80°C; meanwhile, the viscosity for P(S:AN) with 20:80 wt%:wt% is constant at 2.1 Pa·s (±200 MPa·s) until 105°C. Polymeric solutions with low solids content were discarded for later experiments, because they presented low viscosities close to 200 MPa·s. It has been reported that these viscosity values can induce to voids and pores inside the spun fibers or produce a thin polymeric film, converting the electrospinning into electrospray technique.[50,51]

The η values obtained at 8 and 10 wt% of solids content were close to 2 and 10 Pa·s, respectively. Some works have reported range $1 < \eta/\text{Pa·s} < 12$ is appropriate for solutions used in electrospinning techniques. These values of viscosity allow to polymeric chains improve their ability to resist electric field stretching and give stability to the jet.[52–54] In contrast, a very high viscosity in the polymeric solution ($\eta \geq 20$ Pa·s) produces pressure into the needle during electrospinning, leading to bead formation into the fibers, or even clogging the needle tip.[50,55–57]

On the other hand, a sudden increment in viscosity for four solutions is observed reaching values close to 900 Pa·s (Figure 3a) between $88.4 < T/°C < 92.5$°C. This change is attributed to the polymer glass transition (T_g) temperature range, which has been reported from 85° to 95°C for PAN at 10°C/min.[58] These results were corroborated calculating the theoretical T_g by means of Fox equation and the results are shown in Table 3.[59]

3.1 | Fiber morphology

Yarns were fabricated in an electrospinning equipment and collector own made. An electrospinning chamber was designed and built to maintain constant parameters as: temperature, humidity, and minimize the electrostatic forces generated by the nearby electronic devices. A scheme and diagrams of the system made are presented in Supporting Information (Figures S3–S5).

The electrospun fibers were obtained from polymeric solutions with a solids content of 10 wt%, for Series *A* and *B* with different concentrations ratio 0:100, 20:80, 40:60, and 50:50 wt%:wt%. The applied voltage and work distance were maintained constant at 18 kV and 6 cm, respectively. The feed rate for polymeric solution was changed from 0.5, 1.0, and 2.5 ml/hr. Fibers were collected on aluminum foil and dried at 60°C in oven.

Figure 4 shows an SEMs of fibers made of P(S:AN) 20:80 wt%:wt% as example, because all samples presented almost the same physical characteristics. Three fibers bunch with different feed rates are shown, where an increment on average fibers diameter is observed as function of feed rate. For example, 0.5 ml/hr feed rate produces fibers with average diameter of 4.12 μm, while 2.5 ml/hr rate generates fibers with 6.03 μm. The increase

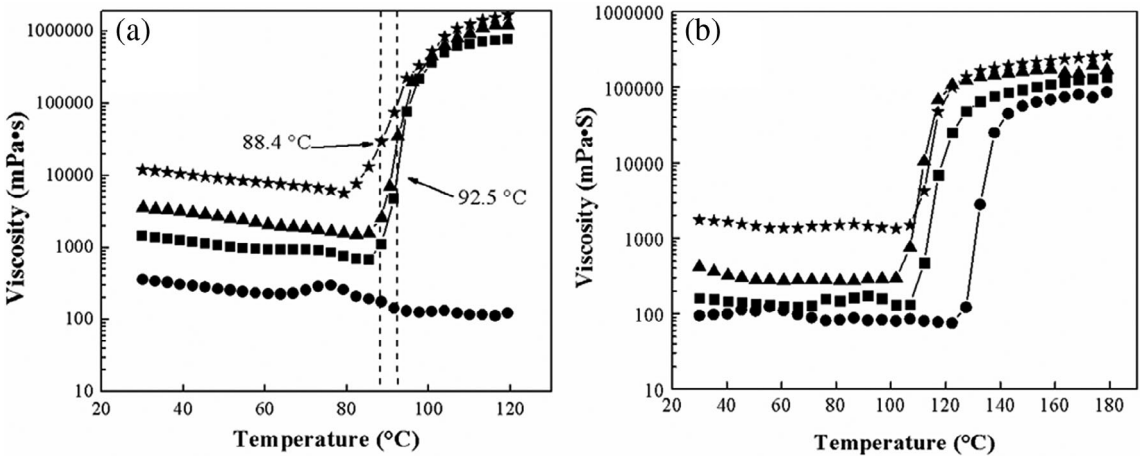

FIGURE 3 Polymeric solutions viscosity at four different ratio concentrations of poly(styrene-*co*-acrylonitrile) P(S:AN) wt%:wt% with (a) (0:100) and (b) (20:80): 4 wt% (●); 6 wt% (■); 8 wt% (▲); and 10 wt% (★)

in feed rate means an increment in the amount of polymeric solution in the needle tip, which widen the Taylor's cone diameter and leads to a bigger fiber diameter.[18,60]

Additionally, small beads are observed on fibers surface at low feed rates (Figure 4a,b), while at 2.5 ml/hr rate, a fiber clean and smooth is found (Figure 4c). These scraps are also attributed to the quantity of polymeric solution in the needle tip. As greater is the amount of polymer solution in the Taylor's cone, as bigger is the number of bonds and strength between the molecules into polymer solution. This means a major cohesive force.[61] At small amounts of polymeric solution, the electric field strength is able to break out it into nanodroplets (as electrospray technique) which cause that they are deposited over the fibers.[51,62] This effect is also presented in materials with a low conductivity and therefore low dielectric constant as polystyrene ($\varepsilon = 2.7$).[63,64]

Figure 5 presents micrographs of fibers with PAN 100 wt%. The micrographs show a fiber bunch with homogeneous and smooth surfaces, free of any scraps. This is associated with the dielectric constant. Where PAN dielectric constant is almost 10 times bigger than polystyrene ($\varepsilon = 21.2$).[65–67]

TABLE 3 Theoretical glass transition temperature for different polymer composition ratios

P(S:AN) (wt%:wt%)	Theoretical T_g (°C)
0:100	91.03
20:80	93.72
40:60	96.47
50:50	97.86

Abbreviation: P(S:AN), poly(styrene-*co*-acrylonitrile).

3.2 | Elastic modulus yarn analysis

A yarn configuration of fibers for Series *A* and *B* was obtained using a blade collector into electrospinning

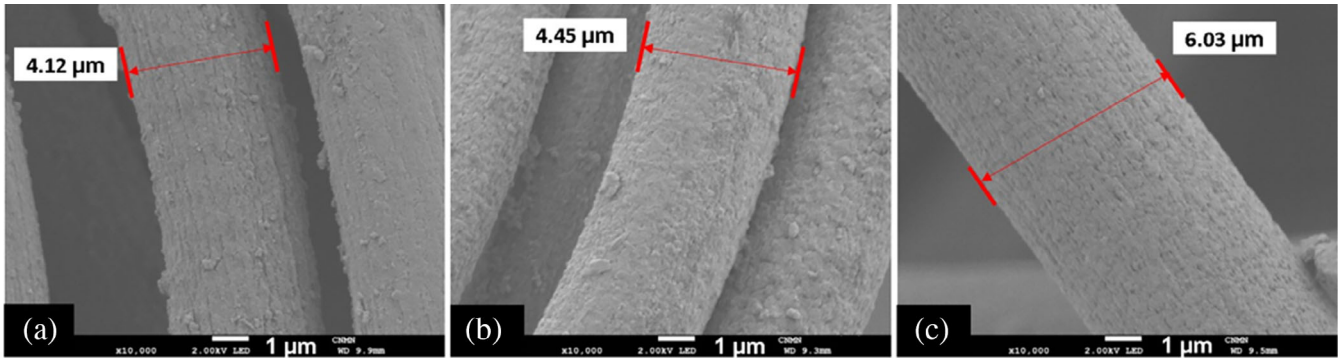

FIGURE 4 Scanning electron microscope (SEM) micrographs of poly(styrene-*co*-acrylonitrile) P(S:AN) 20:80 wt%:wt% spun-fibers with a solids content of 10 wt% at different feed rates: (a) 0.5, (b) 1.5, and (c) 2.5 ml/hr [Color figure can be viewed at wileyonlinelibrary.com]

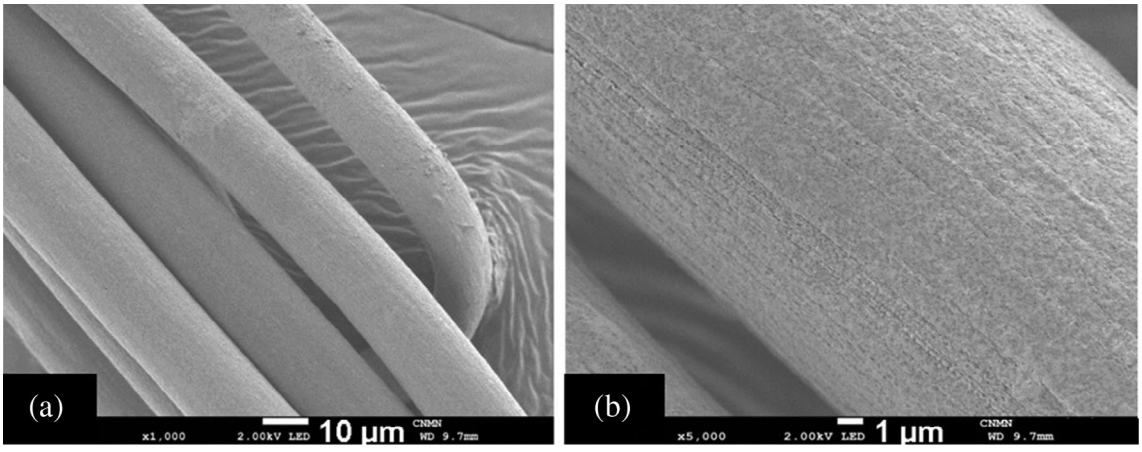

FIGURE 5 Scanning electron microscope (SEM) micrographs of poly(styrene-*co*-acrylonitrile) P(S:AN) 0:100 wt%:wt% spun-fibers with a solid content of 10 wt% at different feed rates: (a) 0.5 and (b) 2.5 ml/hr

process. The fabrication parameters for all samples were: feed rate 2.5 ml/hr, voltage applied 18 kV, and work distance 6 cm. The fibers were deposited overlapping and coiling each other punctually, obtaining fiber yarns with average length of 20 cm and average diameter of 0.8 mm.

TABLE 4 Code for yarns as function of monomeric composition ratio

Series *A*		Series *B*	
Code	P(S:AN) (wt%:wt%)	Code	P(S:AN-AA) (wt%:wt%-wt%)
*A*1	0:100	*B*1	0:100–1
*A*2	20:80	*B*2	20:80–1
*A*3	40:60	*B*3	40:60–1
*A*4	50:50	*B*4	50:50–1

Abbreviations: P(S:AN), poly(styrene-*co*-acrylonitrile); P(S:AN-AA), P(S:AN-acrylic acid).

The yarns obtained were dried in an oven at 60°C by 30 min and cut into 6 cm length pieces.

Stress force as a function of yarn deformation was measured in a texturometer TA.X2i for Series *A* and *B* yarns. Table 4 shows the codification used for the yarns.

Figure 6 shows the curves of tensile strength yarn behavior of Series *A* (Figure 6a) and *B* (Figure 6b). The results show the stress resistance increased as function of acrylonitrile concentration into the polymeric yarns for both series. The highest stress values were obtained to P(S:AN) 0:100 wt%:wt% and P(S:AN-AA) 0:100–1 wt%:wt%-wt% (37 and 19 MPa, respectively).

From the Series *A* plot, three zones are observed: (a) elastic zone (the straight line with a defined slope), where the deformation is proportional to stress; (b) plasticity zone (the increasing and decreasing curve), attributed to irreversible deformation and the process of uncoiled fibers; and (c) the rupture zone (the sudden fall of

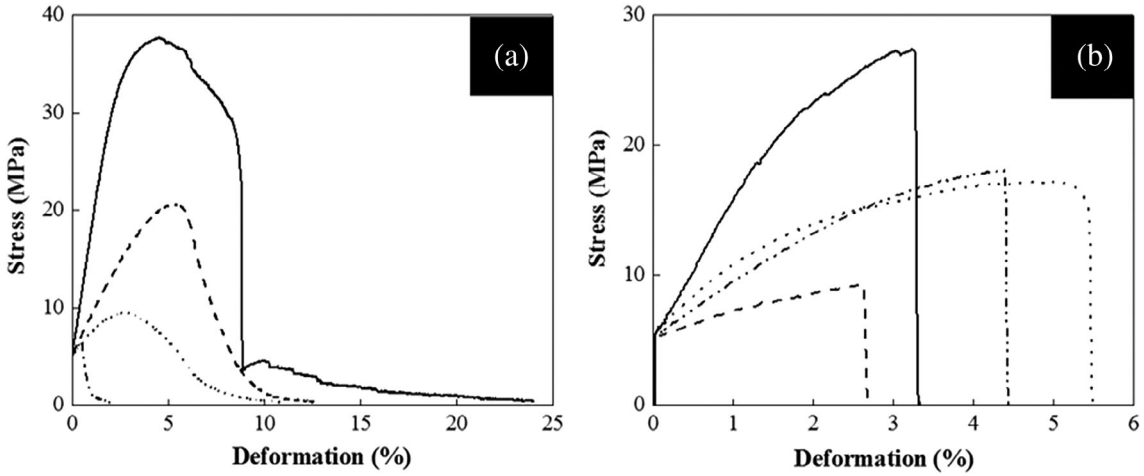

FIGURE 6 Curve stress as a function of deformation, (a) Series *A* and (b) Series *B* yarns: yarn *A*1/*B*1 (—), yarn *A*2/*B*2 (- -), yarn *A*3/*B*3 (··), and yarn *A*4/*B*4 (-·-·)

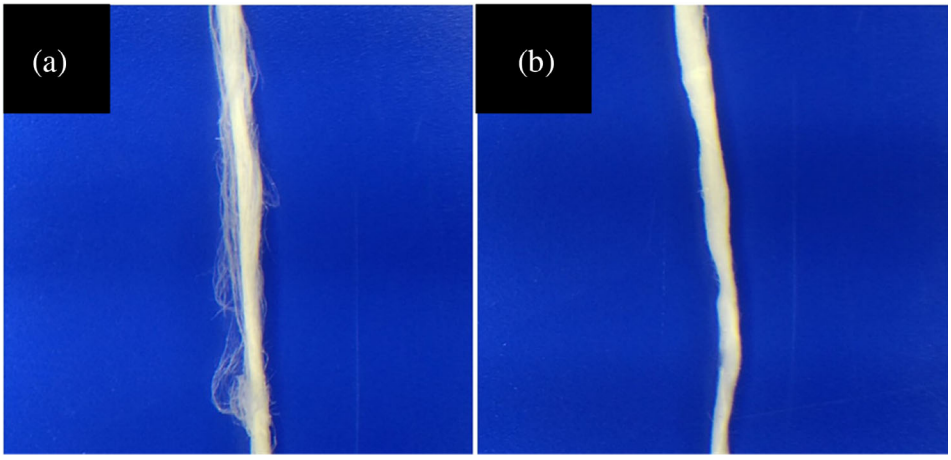

FIGURE 7 Photograph of yarns: (a) Series *A*3 and (b) Series *B*3 [Color figure can be viewed at wileyonlinelibrary.com]

the curve), where the complete break of yarn is observed.[68] The results of yarns plot with AA do not show the plasticity zone because the yarns do not generate an initial opposition to be deformed. This behavior can be attributed to the way of yarns are aligned by the blade collector.

Figure 7 shows a photograph of the coiling obtained for the yarns. Free fibers around the yarn for Series *A*3 are observed (Figure 7a); meanwhile, a yarn with good tangled fibers for Series *B*3 is shown (Figure 7b). These arrangements in the yarn could explain the mechanical behavior; Series *A* shows a gradual breaking yarn, observed by a decreasing curve and attributed to continuous breaking fibers. This could mean the presence of independent fibers into the yarn could produce a less tangle among the fibers and an elastomeric behavior can be observed. Not so in the case of Series *B*, where a punctual break yarn is observed by the vertical straight line at the final curve. This behavior is according with found by Li et al., who mixed PS:PAN. They found that fibers mechanical properties improved by incorporation of PAN in the polymer concentration and reported higher values of break strength (9.15 MPa) and elongation at break (356.74%) compared with PS fibers.[69]

The elastic modulus (*E*) was calculated from the straight line of elastic zone, the slope corresponds to the elastic modulus.[70] The results of yarns elastic modulus as function of polymer composition are presented in Figure 8. The curves show an increment on elastic modulus as acrylonitrile increases into the polymer chains. The elastic modulus for yarns with 20:80 and 40:60 wt%:wt%

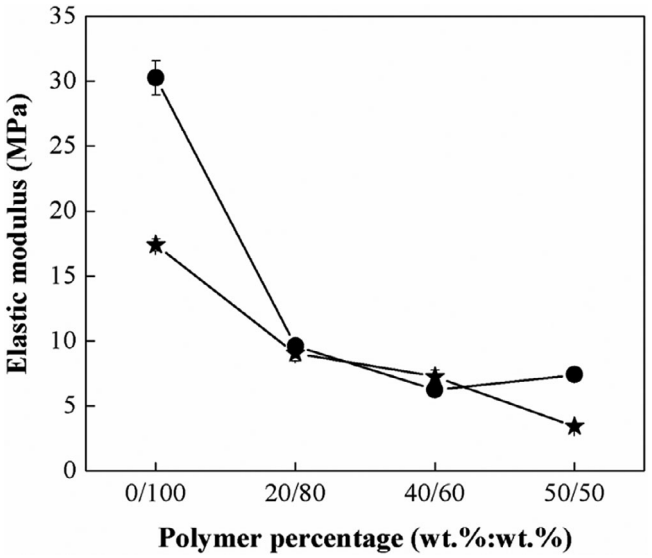

FIGURE 8 Curve elastic modulus yarn Series *A* and *B* as a function of polymer percentage: Series *A* (●) and Series *B* (★)

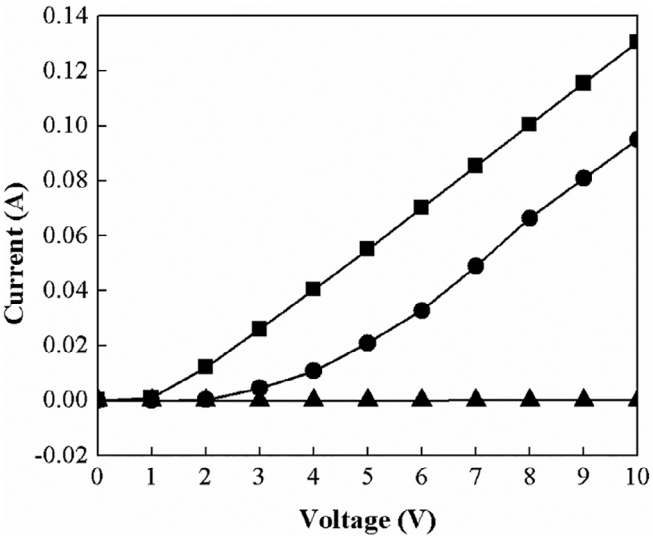

FIGURE 10 Curve current as a function of voltage: saline solution (■); *B*1 yarn moisten (●) and *B*1 yarn dry (▲)

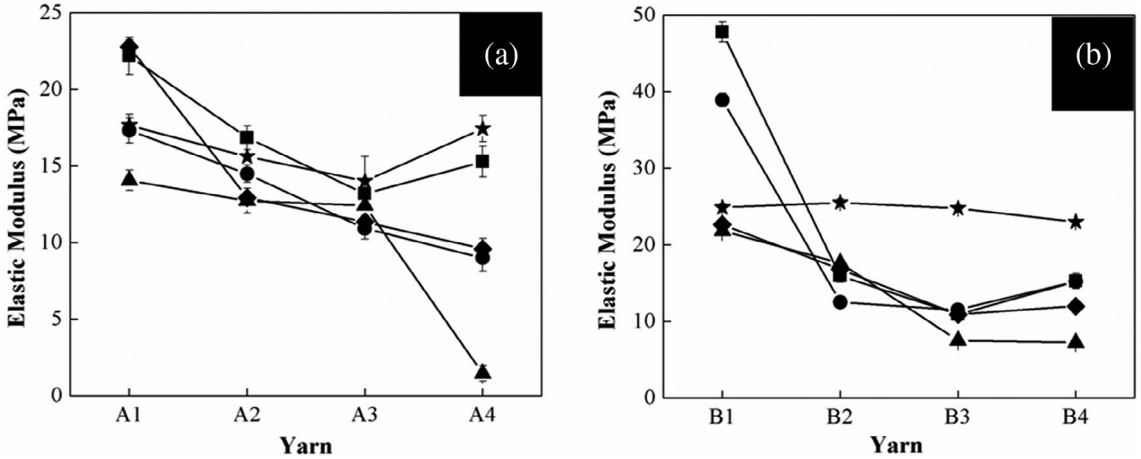

FIGURE 9 Curve elastic modulus (a) Series *A* and (b) Series *B* yarns as a function of polymer percentage with degradation test: 1 day (■); first week (●); second week (▲); third week (◆), and fourth week (★)

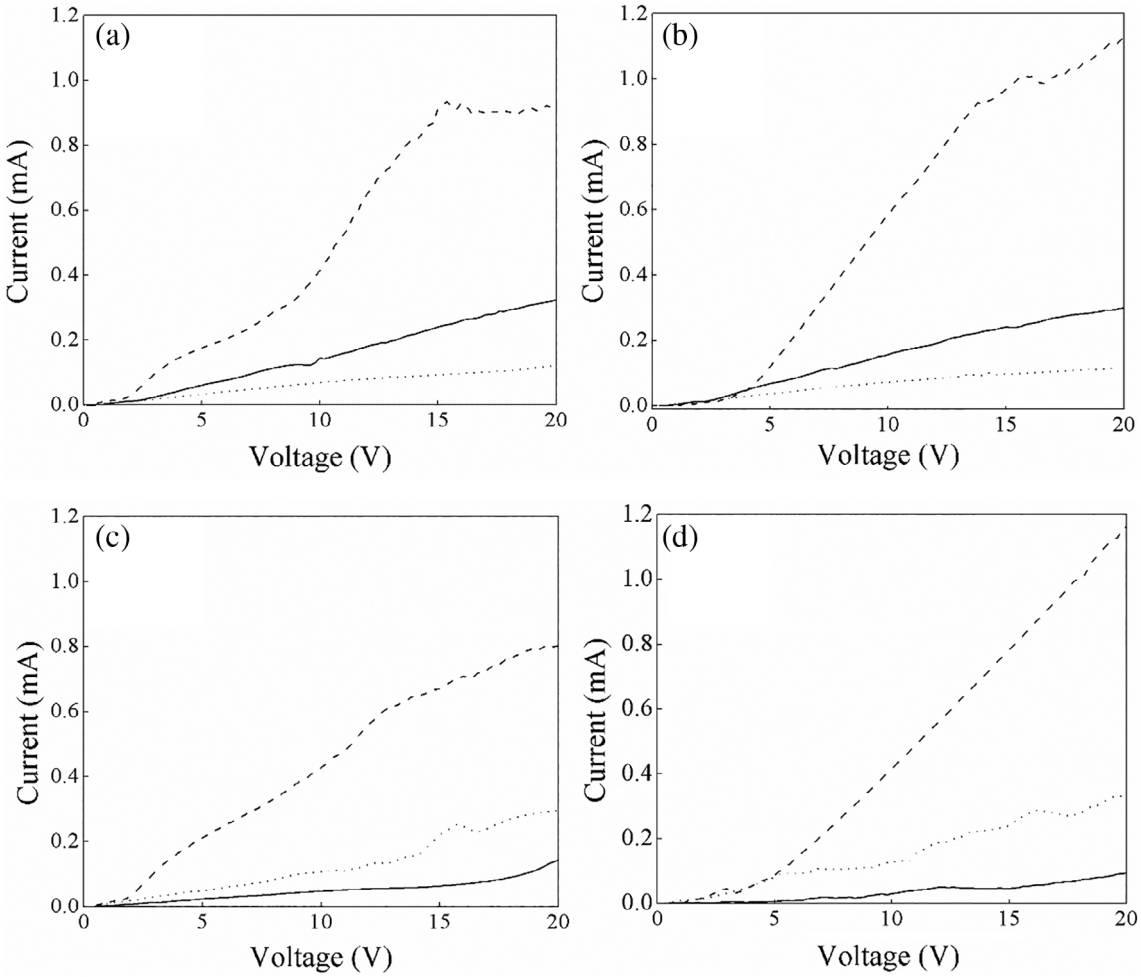

FIGURE 11 Current as function of voltage for yarns poly(styrene-*co*-acrylonitrile) P(S:AN) wt%:wt%: (a) 0:100, (b) 20:80, (c) 40:60, and (d) 50:50 at different pHs: 4 (—), 7 (- -), and 10 (· ·)

were close to 9 and 6 MPa, respectively, for both series. The results also show that yarns have an elastic modulus $20 < E/\text{MPa} < 40$ times bigger than elastic modulus for human tendons, which corresponds to values close to 210 kPa.[71]

The mechanical performance of polymeric yarns can be evaluated by comparison with biological muscle and materials reported in other works. For example, a material made with PAN nanofibers replicates the strain production of skeletal muscle, however the elastic modulus obtained was low (0.207 MPa).[5] Della et al. reported a mechanical performance analysis of a conducting polymer film actuator made of PPy. The results showed a maximum elastic modulus of 3.25 MPa, which corresponds to the highest film thickness used (32 μm).[72] In another work, PAN gel fibers were purchased. These fibers were able to contract to half their initial length with chemical activation, the elastic modulus obtained was 3.9 MPa.[10] The results reported for elastic modulus in these works are below average from present work, where copolymeric yarns present up to 9 MPa. This represents a potential use as material for linear actuators.

3.3 | Elastic modulus yarn analysis after degradation process

The yarns were submitted to degradation process and their mechanical properties were evaluated again. The yarns from Series *A* and *B* were moistened into saline solution (pH = 7) during a month. Samples were taken at several time intervals (1 day, 1–4 weeks) and were dried at 60°C. The yarns were evaluated in the texturometer to obtain the elastic modulus.

Figure 9 shows the elastic modulus as function of polymer composition of yarns for Series *A* and *B* after the degradation process. The highest values for elastic modulus correspond to *A*1 and *B1* yarns moisten 1 day (22 and 48 MPa, respectively), while the *A*4 and *B*4 yarns moisten for 2 weeks get the lowest values (1.5 and 7.3 MPa, respectively).

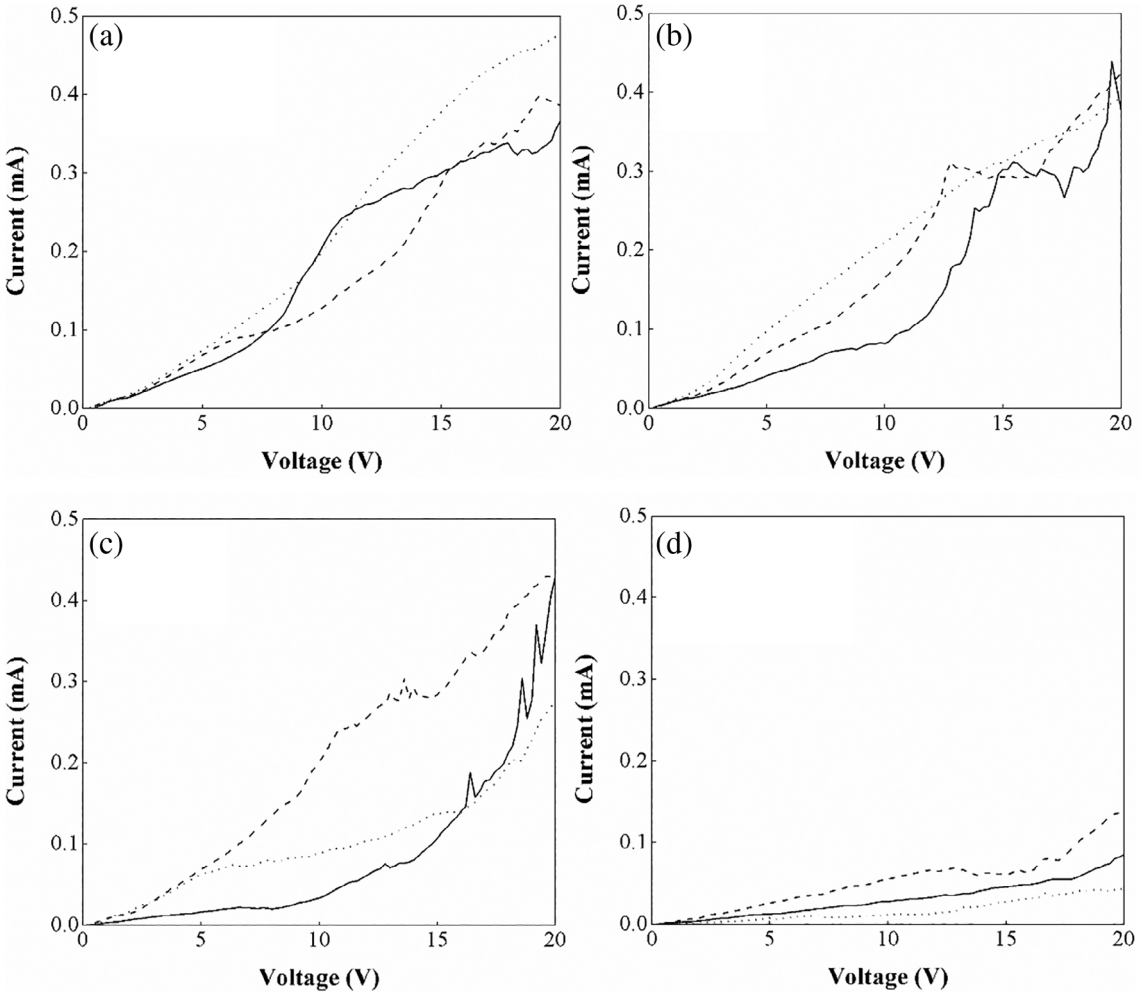

FIGURE 12 Current as function of voltage for yarns P(S:AN-acrylic acid) P(S:AN-AA) wt%:wt%-wt%: (a) 0:100–1, (b) 20:80–1, (c) 40:60–1, and (d) 50:50–1 at different pH: 4 (—), 7 (- -), and 10 (· ·)

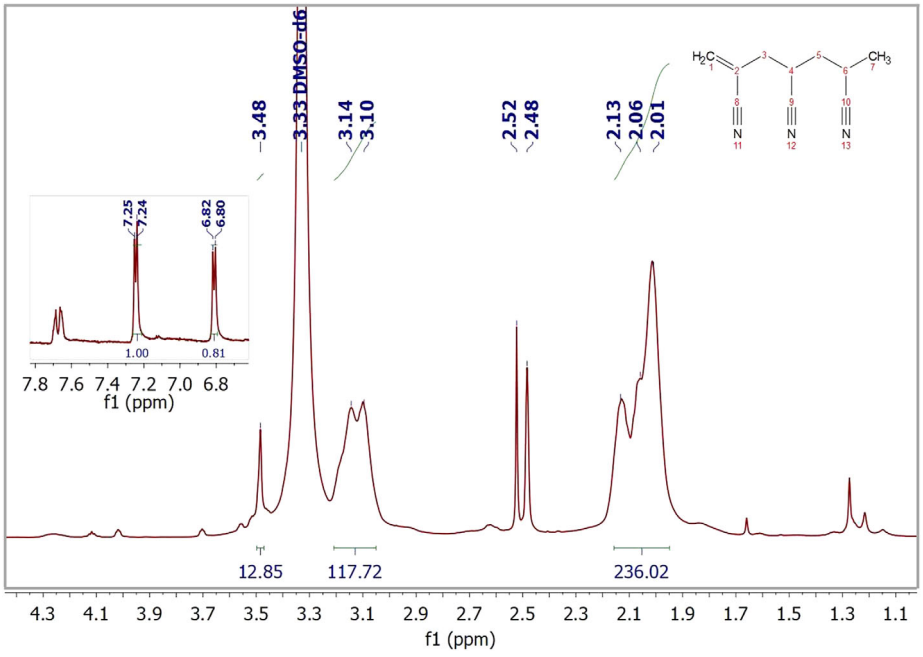

FIGURE 13 ^{1}H NMR of polyacrylonitrile yarn of 1 day submerged [Color figure can be viewed at wileyonlinelibrary.com]

In general, PS has an influence on the elastic modulus loss during the degradation process, except to fourth week where the elastic modulus had a higher value. That is, Series *A* presented values close to 17 MPa while yarns with AA had values close to 25 MPa. This elastic modulus value was higher than yarns moisten for 2 and 3 weeks. The improvement into the elastic modulus can be attributed to the loss of short polymeric chains from yarns to the saline solution and may be that the exchange of carboxylic groups with Na^+ allows a strengthening of the yarn structure. This result implicates that the materials keep a high elastic modulus, when they are moistened into saline solution for a large time.

3.4 | Electrical behavior on moisten yarns

The yarns mechanical properties could allow them to have reversible contraction or elongation states (volumetric or length). These mechanical changes can be generate and/or controlled by electric pulses. For this reason, the yarns electrical behavior (Series *A* and *B*) were evaluated into an electrical station and the experiments were made by quadruplicate. Curves voltage as a function of current was measured for moisten yarns with saline solution. The saline solution and dry yarn were used as reference.

The results are shown in Figure 10 for yarn *B*1 P(S:AN-AA) (0:100–1 wt%:wt%-wt%) measured at 7.0 pH as example. It is notorious that saline solution gets a proportional current increment as the voltage increase, characteristic of a conductor material. The dry fiber presents an insulator behavior; meanwhile, the moisten fiber shows a current increment almost linear from 4 V. This means that the saline solution turn the fiber to a "semiconductor material."

For next experiments, the saline solution pH was changed with buffer solutions (4, 7, and 10 pH) and the yarns were moistened for electrical evaluation.

The electric behavior of yarns Series *A* are shown in Figure 11. Yarns Series *A* moistened with saline solution at 7 pH showed the highest conductivity with values close to 1.2 mA ± 0.35 mA. The curves at 7 pH presented zones with lineal conductivity and a dependence to styrene concentration. P(S:AN), for 50:50 wt%:wt% shows a defined slope from 5 V (Figure 16d). This phenomenon could be attributed to electron relocation from acrylonitrile and aromatic ring of styrene causing by the electric current applied as occurs in PANi case, where the free energy gain by delocalization of the π-electrons in the chain is balanced by the

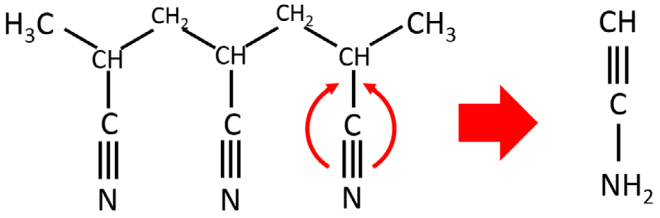

FIGURE 14 Representation of electrons dislocation forming triple bond (—CH≡C—) [Color figure can be viewed at wileyonlinelibrary.com]

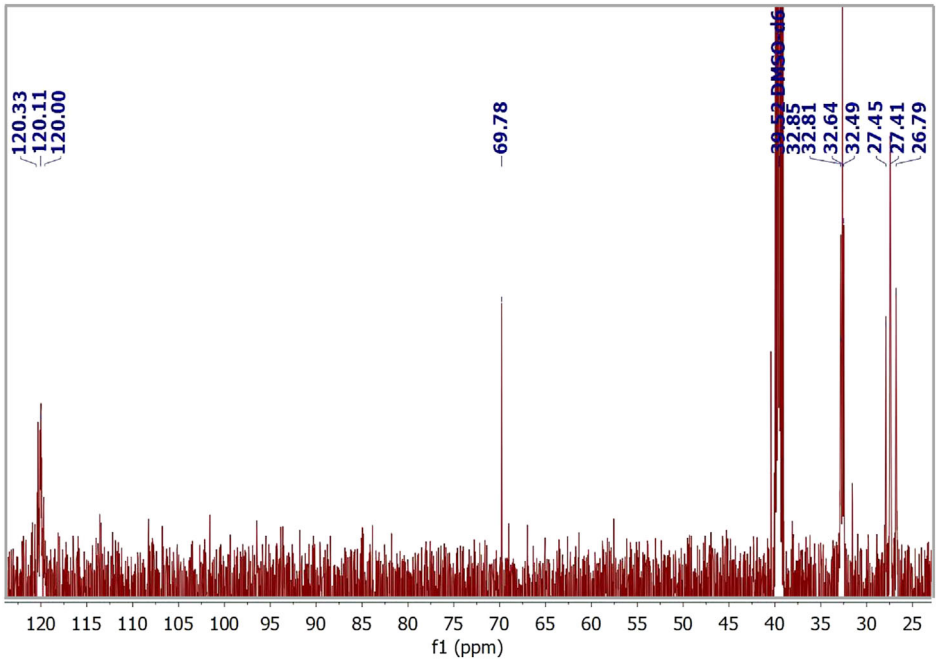

FIGURE 15 ^{13}C NMR of polyacrylonitrile yarn of 1 day submerged in NaCl solution [Color figure can be viewed at wileyonlinelibrary.com]

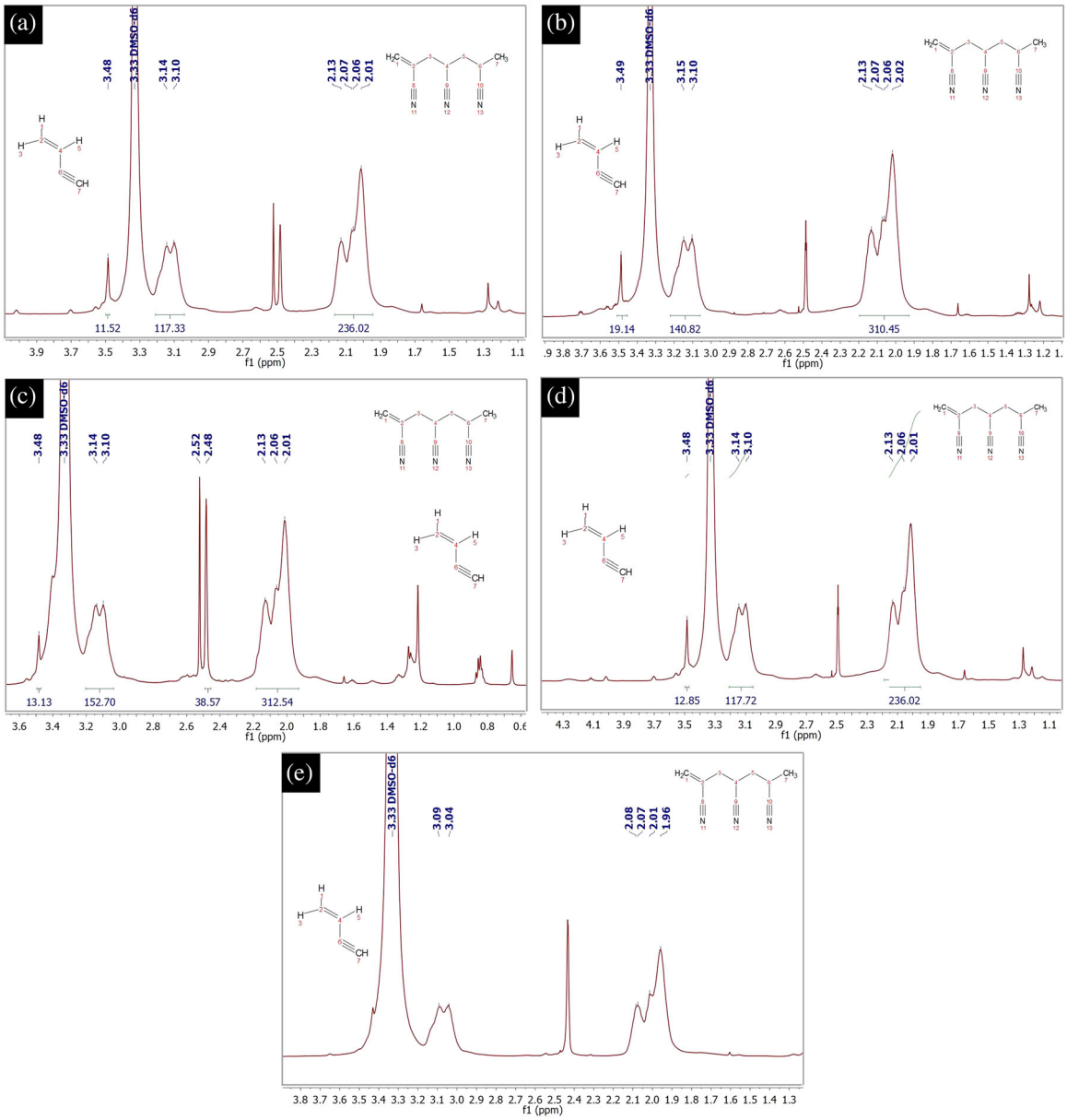

FIGURE 16 ^{1}H NMR of polyacrylonitrile yarn at different submerged times: (a) 15 days, (b) 10 days, (c) 5 days, (d) 1 day, and (e) 0 days [Color figure can be viewed at wileyonlinelibrary.com]

loss of energy due to steric effects in planar conformations, reaching a current by electron relocation. Therefore, the material can be transformed from an insulating state to a conducting state by protonation of the product prepared.[73,74]

Figure 12 shows a voltage–current curve for Series *B* moisten at different pH in the saline solution. The results show the maximum current values are close to 0.4 ± 0.05 mA, which is less than Series *A*. This could be explained because the AA could act as resistance into the polymer chain, reducing the electron relocation by resonance effects and causing a decrease of current.

3.5 | ^{1}H-NMR and ^{13}C-NMR analysis

The chemical structure of PAN yarn P(S:AN) 0:100 wt%: wt% of 1 day submerged was confirmed by ^{1}H-NMR (Figure 13). Wide multiple signals at $\delta = 2.1$ ppm and at $\delta = 3.1$ ppm corresponding to methylene (—CH_2—) and methine (—CH—) protons, respectively, from PAN are shown.[75] The wide signals are attributed to the interaction between polymeric chain and sodium ions from saline solution.[76]

A small single signal is presented at $\delta = 3.48$ ppm attributed to the formation of a triple bond (—CH≡C—) due to dislocation of free electrons from nitrogen which

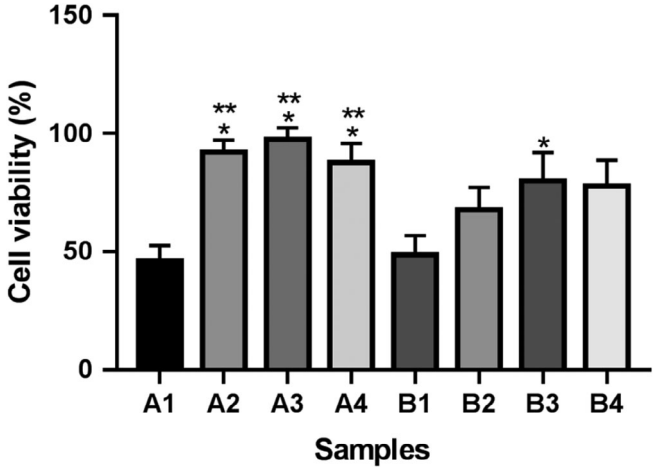

FIGURE 17 Cell viability percentage of yarns Series *A* and *B* on macrophage

confirms the electrical properties results (Figure 14). Finally, two doublet signals are shown at $\delta = 6.82$ and $\delta = 7.25$ ppm attributed to alkene protons located at beginning and end of the chain.

The same PAN sample was also analyzed by ^{13}C NMR (Figure 15). The signals at $\delta = 27.41$ ppm correspond to methine carbon, $\delta = 32.81$ ppm to the methylene carbon, $\delta = 69.78$ ppm to triple bond carbon and a multiple signals at $\delta = 120.11$ ppm to the nitrile group.[77] These results corroborate the triple bond, consequence of electrons dislocation of nitrogen.

The interaction between yarns and saline solution, when they were submerged at different periods of time was analyzed by ^{1}H NMR (Figure 16). The spectra show that samples with 15 days of immersion time (Figure 16a) had the lowest intensity in the principal signals (—CH_2— and —CH—), while the highest signal intensity corresponds to 1 day of immersion (Figure 16d), it could be due to major interaction between these groups and sodium ions from saline solution, resulting in signals wider and shorter.

3.6 | Toxicological evaluation

The cell proliferation test was performed using macrophage cell line J774A.1 (mouse macrophages). The cell line were inoculated at a density of 200,000 cells per well on to 24-well plates containing the Series *A* and *B* yarns. The cytotoxic effect of samples was evaluated by MTT assay by duplicate and the results are shown in Figure 17. Bars represent the means and standard deviation of two independent experiments. The data were analyzed with one-way analysis of variance, with Tukey's posttest.*$p < .05$ represents the significant differences of all samples compared with yarn *A*1, while **$p < .05$ indicates the significant differences of all samples compared with yarn *B*1.

The samples with PAN and P(AN-AA) have an important decrease of cell viability (approximate 50%). The increment of styrene into the yarns (*A2* and *A3* samples) enhanced the cell viability, reaching values close to 100%. In general, Series *B* had a decrement of cell viability compared with Series *A*, which means that the presence of acrylic acid in the sample reduce the cells growth.

The cytocompatibility between cells and copolymers is affected by type of present functional groups in the material. In this case, the group —COOH from acrylic acid (Series *B*) generated a toxic effect over the macrophages. The presence of acrylic acid in the polymer is demonstrated with a low pH (5), while Series *A* have a pH (6–7).[78,79]

4 | CONCLUSIONS

The polymers used in the fabrications of yarns P(S:AN) and P(S:AN-AA) were synthesized by emulsion polymerization techniques changing the composition of polymer. Electrospinning equipment was built and yarns with 20 cm of length were collected using a blade collector own made. The mechanical properties tests showed an influence of acrylonitrile composition increasing the elastic module of yarns reaching values up to 40 MPa for PAN. The mechanical characterization of yarns after degradation process using saline solution indicated that, AA allowed keeping a constant elastic modulus at long times and sodium ions strengthened the yarns structure. The yarn polymeric concentration 50:50 wt%:wt% showed an increment in the electric current up to 1.2 mA, attributed to free electron relocation from nitrile group (PAN) into polymeric chain. This was confirmed after ^{1}H-NMR and ^{13}C-NMR spectra, where a signal at 3.48 ppm appears, which belongs to (—CH≡C—) complex generated by electron relocation. Cell viability assays showed that yarns with AA reach up to viability 80%, meanwhile yarns without AA reached values close to viability 100%. The presented results indicate that polymeric yarns have a potential to be used as artificial muscle or actuators, further experiments are needed to confirm this behavior.

ACKNOWLEDGMENTS

This work was supported by a grant from Consejo Nacional de Ciencia y Tecnología (CONACyT, grant 596936) and Secretaria de Investigación y Posgrado, Instituto Politécnico Nacional (SIP-IPN, projects

20195353 and 20196644). R.C.B. thanks for the BEIFI scholarship granted from PIFI. The authors would like to acknowledge to Centro de Nanociencias y Micro y Nanotecnologías (CNMN) from Instituto Politécnico Nacional for SEM assays.

ORCID

Mónica Corea https://orcid.org/0000-0001-5589-701X

REFERENCES

[1] H. Fujisue, T. Sendai, K. Yamato, W. Takashima, K. Kaneto, *Bioinspir. Biomim.* **2007**, *2*, S1.
[2] M. Bassil, J. Davenas, M. El Tahchi, *Adv. Sci. Technol.* **2008**, *61*, 85.
[3] K. Choe, K. J. Kim, *Sens. Actuat. A: Phys.* **2006**, *126*, 165.
[4] J. Fan, G. Li, *RSC Adv.* **2017**, *7*, 1127.
[5] M. A. Gonzalez, W. W. Walter, *Electroact. Polym. Actuat. Dev.* **2014**, *9056*, 90563J1.
[6] S. M. Mirvakili, I. W. Hunter, *Adv. Mater.* **2018**, *30*, 1704407.
[7] S. Yahara, S. Wakimoto, T. Kanda, K. Matsushita, *Sens. Actuat. A: Phys.* **2019**, *295*, 637.
[8] R. P. Reed, R. E. Schramm, A. F. Clark, *Cryogenics* **1973**, *13*, 67.
[9] E. Smela, *Adv. Mater.* **2003**, *15*, 481.
[10] H. B. Schreyer, N. Gebhart, K. J. Kim, M. Shahinpoor, *Biomacromolecules* **2000**, *1*, 642.
[11] G. Morari, in *Advances in Conducting Polymers Research*, 4th ed. (Ed: L. Michaelson), Nova Science Publishers, Inc., New York, NY **2015**, p. 3.
[12] S. Bhaskar, J. Lahann, *J. Am. Chem. Soc.* **2009**, *131*, 6650.
[13] K. Cho, H. J. Lee, S. W. Han, J. H. Min, H. Park, W. Koh, *Angew. Chem. Int. Ed. Engl.* **2015**, *54*, 11511.
[14] G. Zhou, G. Yang, X. Li, B. Chen, J. Fan, H. Hou, S. Zhou, *Appl. Mater. Interfaces* **2018**, *10*, 14276.
[15] N. Bhardwaj, S. C. Kundu, *Biotechnol. Adv.* **2010**, *28*, 325.
[16] G. Panthi, M. Park, H. Y. Kim, S. J. Park, *J. Ind. Eng. Chem.* **2015**, *24*, 1.
[17] A. Bara, E. Chitanu, C. Banciu, et al. Polyacrylonitrile-based electrospun fibers. 2015 9th International Symposium on Advanced Topics in Electrical Engineering. **2015**, 250–253.
[18] N. H. A. Ngadiman, M. Y. Noordin, A. Idris, D. Kurniawan, *Adv. Mater. Res.* **2013**, *845*, 985.
[19] R. Khajavi, M. Abbasipour, *Electrospun Nanofibers*, Elsevier Ltd., Cambridge, UK **2016**, p. 109.
[20] D. B. R. Silva, L. P. C. Júnior, M. F. de Aguiar, et al., *J. Mol. Liq.* **2018**, *272*, 1070.
[21] N. Savest, T. Plamus, K. Kütt, U. Kallavus, M. Viirsalu, E. Tarasova, V. Vassiljeva, I. Krasnou, A. Krumme, *J. Electrostat.* **2018**, *96*, 40.
[22] M. Ranjbar-Mohammadi, M. Zamani, M. P. Prabhakaran, S. H. Bahrami, S. Ramakrishna, *Mater. Sci. Eng. C* **2016**, *58*, 521.
[23] N. Sarier, R. Arat, Y. Menceloglu, E. onder, E. C. Boz, O. Oguz, *Thermochim. Acta* **2016**, *643*, 83.
[24] S. Rahmani, A. Arefazar, M. Latifi, *Mater. Res. Express* **2017**, *4*, 1.
[25] G. Moradi, S. Zinadini, L. Rajabi, S. Dadari, *Appl. Surf. Sci.* **2018**, *427*, 830.
[26] I. P. Dobrovolskaya, I. O. Lebedeva, V. E. Yudin, P. V. Popryadukhin, E. M. Ivan'kova, V. Y. Elokhovskii, *Polym. Sci. Ser. A* **2016**, *58*, 246.
[27] X. Chen, H. Yan, W. Sun, Y. Feng, J. Li, Q. Lin, Z. Shi, X. Wang, *Polym. Bull.* **2015**, *72*, 3097.
[28] I. Esmaeilzadeh, V. Mottaghitalab, B. Tousifar, A. Afzali, M. Lamani, *Int. J. Ind. Chem.* **2015**, *6*, 193.
[29] S. Kwak, A. Haider, K. C. Gupta, S. Kim, I. K. Kang, *Nanoscale Res. Lett.* **2016**, *11*, 323.
[30] Y. Liu, M. Park, H. K. Shin, B. Pant, J. Choi, Y. W. Park, J. Y. Lee, S. J. Park, H. Y. Kim, *J. Ind. Eng. Chem.* **2014**, *20*, 4415.
[31] S. Li, Y. Zhao, C. Wang, D. Li, K. Gao, *Mater. Lett.* **2016**, *170*, 122.
[32] S. G. Leonardi, A. Mirzaei, A. Bonavita, S. Santangelo, P. Frontera, F. Pantò, P. L. Antonucci, G. Neri, *Nanotechnology* **2016**, *27*, 75502.
[33] M. Mondragón, A. S. Garzón, R. Caro, *J. Appl. Polym. Sci.* **2016**, *133*, 44019.
[34] H. Ning, H. Xie, Q. Zhao, J. Liu, W. Tian, Y. Wang, M. Wu, *J. Alloys Compd.* **2017**, *722*, 716.
[35] Z. Cheng, Y. Zhang, Z. Han, L. Cui, L. Kang, F. Zhang, *RSC Adv.* **2016**, *6*, 85545.
[36] M. Castilho, D. Feyen, M. Flandes-Iparraguirre, G. Hochleitner, J. Groll, P. A. F. Doevendans, T. Vermonden, K. Ito, J. P. G. Sluijter, J. Malda, *Adv. Health Mater.* **2017**, *6*, 1700311.
[37] S. Chen, R. Li, X. Li, J. Xie, *Adv. Drug. Deliv. Rev.* **2018**, *132*, 188.
[38] Z. Tan, H. Wang, X. Gao, T. Liu, Y. Tan, *Mater. Sci. Eng. C* **2016**, *67*, 369.
[39] S. L. Chai, M. M. Jin, *J. Appl. Polym. Sci.* **2009**, *114*, 2030.
[40] L. Lei, Q. Zhang, S. Shi, S. Zhu, *J. Colloid. Interface Sci.* **2016**, *483*, 232.
[41] L. A. Puentes, K. M. Gregorio, A. M. Bolarín, M. E. Navarro, et al., *J. Nanopart. Res.* **2016**, *18*, 212.
[42] C. Wohlfarth, in *Static dielectric constants of pure liquids and binary liquid mixtures (supplement to IV/6)* (Ed: M. D. Lechner), Springer, Berlin **2008**, p. 175.
[43] C. L. Winzor, D. C. Sundberg, *Polymer* **1992**, *33*, 3797.
[44] M. R. Muscato, D. C. Sundberg, *J. Polym. Sci. Part B: Polym. Phys.* **1991**, *29*, 1021.
[45] X. Zhang, Y. Sun, Y. Mao, K. Chen, Z. Cao, D. Qi, *RSC Adv.* **2018**, *8*, 3910.
[46] Y. Sun, Y. Yin, M. Chen, S. Zhou, L. Wu, *Polym. Chem.* **2013**, *4*, 3020.
[47] I. Cho, K. W. Lee, *J. Appl. Polym. Sci.* **1985**, *30*, 1903.
[48] E. Limousin, N. Ballard, J. M. Asua, *Prog. Org. Coat.* **2019**, *129*, 69.
[49] C. F. Lee, *Polymer* **2000**, *41*, 1337.
[50] E. A. Morris, M. C. Weisenberger, *ACS Symp. Ser.* **2014**, *1173*, 189.
[51] D. Li, Y. Xia, *Adv. Mater.* **2004**, *16*, 1151.
[52] S. K. Nataraj, K. S. Yang, T. M. Aminabhavi, *Prog. Polym. Sci.* **2012**, *37*, 487.
[53] L. Mei, H. Chen, Y. Shao, et al., *High Perform. Polym.* **2018**, **31**, 230.
[54] C. Li, Q. Li, X. Ni, et al., *Materials* **2017**, *10*, 572.

[55] E. A. Morris, M. C. Weisenberger, S. B. Bradley, M. G. Abdallah, S. J. Mecham, P. Pisipati, J. E. McGrath, *Polymer* **2014**, *55*, 6471.
[56] S. Moon, J. Choi, R. J. Farris, *Fibers Polym.* **2008**, *9*, 276.
[57] P. E. Rouse, *J. Chem. Phys.* **1953**, *21*, 1272.
[58] R. Hiorns, in *Polymer Handbook*, 4th ed. (Eds: J. Brandup, E. H. Immergut, E. A. Grulke, A. Abe, D. R. Bloch), John Wiley and Sons, New York, NY **1999**, p. 2250.
[59] T. G. Fox, P. J. Flory, *J. Appl. Phys.* **1950**, *21*, 581.
[60] S. Ramakrishna, K. Fujihara, W. E. Teo, et al., *An introduction to electrospinning and nanofibers*, World Scientific, Singapore **2005**, p. 103.
[61] J. B. Rosenholm, K. E. Peiponen, E. Gornov, *Adv. Colloid Interface Sci.* **2008**, *141*, 48.
[62] T. Gesang, W. Possart, O. D. Hennemann, J. Petermann, *Langmuir* **1996**, *12*, 3341.
[63] C. J. Luo, E. Stride, M. Edirisinghe, *Macromolecules* **2012**, *45*, 4669.
[64] P. Debye, F. Bueche, *J. Phys. Colloid Chem.* **1951**, *55*, 235.
[65] S. Madakbaş, Z. Çelik, F. Dumludağ, M. V. Kahraman, *Polym. Bull.* **2014**, *71*, 1471.
[66] L. Wannatong, A. Sirivat, P. Supaphol, *Polym. Int.* **2004**, *53*, 1851.
[67] M. M. Hohman, M. Shin, G. Rutledge, M. P. Brenner, *Appl. Phys. Fluids* **2001**, *13*, 2221.
[68] G. Wang, D. Yu, A. D. Kelkar, L. Zhang, *Prog. Polym. Sci.* **2017**, *75*, 73.
[69] P. Li, Y. Qiao, L. Zhao, D. Yao, H. Sun, Y. Hou, S. Li, Q. Li, *Mar. Pollut. Bull.* **2015**, *93*, 75.
[70] H. Ku, H. Wang, N. Pattarachaiyakoop, M. Trada, *Compos. Part B: Eng.* **2011**, *42*, 856.
[71] B. C. W. Kot, Z. J. Zhang, A. W. C. Lee, et al., *PLoS One* **2012**, *7*, 2.
[72] A. Della Santa, D. De Rossi, A. Mazzoldi, *Synth. Metals* **1997**, *90*, 93.
[73] T. Hjertberg, M. Sandberg, O. Wennerström, I. Lagerstedt, *Synth. Met.* **1987**, *21*, 31.
[74] S. Stafström, J. L. Brédas, *Synth. Metals* **1986**, *14*, 297.
[75] M. Minagawa, K. Ute, T. Kitayama, K. Hatada, *Macromolecules* **1994**, *27*, 3669.
[76] F. Deng, G. Wang, Y. Du, et al., *Solid State Nucl. Mag. Reson.* **1997**, *7*, 281.
[77] K. Katsuraya, K. Hatanaka, K. Matsuzaki, M. Minagawa, *Polymer* **2001**, *42*, 6323.
[78] W. Luo, J. Cai, X. Zhu, L. Huang, Z. Xu, P. Cen, *Eng. Life Sci.* **2012**, *12*, 1.
[79] C. Yahata, J. Suzuki, A. Mochizuki, *J. Bioact. Compat. Polym.* **2019**, *34*, 1.

SUPPORTING INFORMATION

Additional supporting information may be found online in the Supporting Information section at the end of this article.

How to cite this article: Caro-Briones R, García-Pérez BE, Báez-Medina H, et al. Influence of monomeric concentration on mechanical and electrical properties of poly(styrene-*co*-acrylonitrile) and poly(styrene-*co*-acrylonitrile/acrylic acid) yarns electrospun. *J Appl Polym Sci.* 2020;e49166. https://doi.org/10.1002/app.49166